Sharp interface limit of a phase-field model of crystal grains

Alexander E. Lobkovsky and James A. Warren
National Institute of Standards and Technology, 100 Bureau Drive, Gaithersburg, Maryland 20899
(Received 7 December 2000; published 24 April 2001)

We analyze a two-dimensional phase field model designed to describe the dynamics of crystalline grains. The phenomenological free energy is a functional of two order parameters. The first one reflects the orientational order, while the second reflects the predominantly local orientation of the crystal. We consider the gradient flow of this free energy. Solutions can be interpreted as ensembles of grains (in which the orientation is constant in space) separated by grain boundaries. We study the dynamics of the boundaries as well as the rotation of the grains. In the limit of an infinitely sharp interface, the normal velocity of the boundary is proportional to both its curvature and its energy. We obtain explicit formulas for the interfacial energy and mobility, and study their behavior in the limit of a small misorientation. We calculate the rate of rotation of a grain in the sharp interface limit, and find that it depends sensitively on the choice of the model.

DOI: 10.1103/PhysRevE.63.051605 PACS number(s): 81.10.Aj, 81.30.−t, 81.10.Jt, 61.72.Mm

I. INTRODUCTION

The characterization and evolution of microstructure forms a cornerstone of materials science. In particular, the grain structure of a polycrystalline material determines many of its properties. Recent efforts at modeling the evolution of grain boundaries have used a variety of approaches [1–4]. Herein we focus on the recently introduced phase field model of Kobayashi, Warren, and Carter (KWC) [5] which is based on earlier attempts by the same authors [6,7]. Phase field models have been applied to the problem of solidification, with great success [8–10], but only recently to the problem of grain boundaries. In general, phase field methods continue to show promise in many areas of pattern formation, as they obviate the need to track the interface.

The model is motivated by symmetry principles, and has a surprisingly rich set of physical characteristics. In particular, KWC showed numerically that solutions to this model can be interpreted as a collection of grains. The velocity of the interface between the grains was found to be approximately proportional to the local curvature of the interface, but the grains were also able to rotate toward lower energy misorientations. In support of the notion of grain rotation, three independent unpublished molecular dynamics studies by Upmanyu and Srolovitz, Phillpot and Wolf, and Srinivasan and Cahn, suggested that grain rotation will occur under certain circumstances. In addition, there is a substantial history (and debate) concerning the mechanisms [11–13] and observation of grain rotation [14,15].

The KWC phase field model is mathematically challenging because of a singular term in the free energy. Kobayashi and Giga [16] studied similar singular models, and showed that there is a way to handle the singularity consistently. In this paper we will apply their method to the KWC model, and show that its solutions can indeed be interpreted as grains separated by grain boundaries.

Grain boundaries in a polycrystalline material are narrow compared to the grain size. Therefore, conventionally, grain boundaries are described by sharp interface models [17], in which the boundaries are treated as two-dimensional surfaces. Typically, in these models, a boundary is characterized by an energy and a mobility. These quantities may depend on the misorientation of the adjacent grains and the inclination of the boundary. We should note that one of the original motivations of phase field modeling was the idea that a diffuse interface regularizes the inherently singular nature of the sharp interface models [8]. However, in order to make contact with these sharp interface models, it is often useful to consider the converse: how do diffuse interface models behave in the sharp interface limit?

Thus the main goal of this paper is to analytically obtain the energy and mobility of a grain boundary, as well as the rotation rate of a grain within the KWC model. We accomplish this task by considering a limit of the model parameters in which the width of the boundary vanishes, while its measurable characteristics remain finite and nonzero. The methodology of this so called sharp interface limit is well established [18–20]. There exist cases, such as propagation of fronts into linearly unstable media, for which this procedure is not well defined [21]. However, as will become clear below, the motion of grain boundaries in our model is an example of a front with exponential relaxation, and thus we do not anticipate any difficulties of the sort discussed in Ref. [21].

This paper is organized as follows. In Sec. II we introduce the order parameters, phenomenological free energy, and gradient flow equations. We next perform a formal asymptotic expansion of the model in Sec. III. The zeroth order problem of this expansion is discussed in Sec. IV, where we obtain the profile and the energy of the static flat boundary. In Sec. V, the first order asymptotics are examined. We are able to determine the velocity of a curved grain boundary. We find that this velocity is proportional to both the curvature and the interfacial energy, and we obtain an expression for the mobility of the interface. As noted above, grains can rotate in this model. We calculate the rate of rotation of a grain in Sec. VI. Finally, in Sec. VII, we apply all of the results described herein to the simple case of a circular grain embedded in a matrix. In conclusion, we discuss further ideas, and the implications of this phase field model for the problem of coarsening in polycrystals in Sec. VIII.

II. MODEL

We model the evolution of a collection of nearly perfect crystalline grains in two dimensions via a phase field model. First we discuss order parameters which capture the microscopic physics of grain boundaries. It is then possible to construct a phenomenological free energy which favors a perfect uniform crystal. The structure of the solutions of the gradient flow of this free energy can then be interpreted as an evolving ensemble of grains.

Following Ref. [5], we develop two order parameters. To distinguish grains of different orientations, we introduce a continuously varying local orientation θ. Since the energy of crystal does not depend on θ itself, the phenomenological free energy will be a functional of the gradients of θ only. The second order parameter η is used to differentiate the nearly perfect crystal in the interior of the grains from the disordered material in the grain boundary. It varies from perfect order $\eta=1$ to complete disorder $\eta=0$. Both order parameters are not conserved.

We analyze the free energy (based on KWC)

$$\mathcal{F}[\eta,\theta]=\frac{1}{\epsilon}\int_\Omega dA\left[\frac{\alpha^2}{2}|\nabla\eta|^2+f(\eta)+g(\eta)s\right.$$
$$\left.\times|\nabla\theta|+h(\eta)\frac{\epsilon^2}{2}|\nabla\theta|^2\right], \quad (1)$$

where α, ϵ, and s are positive model parameters. Some readers may find the overall prefactor of $1/\epsilon$ suggestive. Subsequently we will examine the limit $\epsilon\to 0$. This prefactor ensures that the surface energy of a grain boundary tends to a non zero constant.

Term by term, the above free energy deserves some discussion, although the reader interested in the full motivation of this model is referred to Ref. [5]. The first term describes the penalty for gradients in the order parameter (grain boundaries cost energy). The free energy density $f(\eta)$ is chosen to be a single well, with the minimum at $\eta=1$ and $f(1)=0$ reflecting the fact that disordered material has higher free energy. The third and fourth terms are an expansion in $|\nabla\theta|$, where the couplings $g(\eta)$ and $h(\eta)$ must be positive definite. KWC argued that the expansion in $|\nabla\theta|$ must begin at first order to assure the existence of stable grain boundaries. This term yields a singularity in the dynamic equations.

Indeed, Ref. [5] omitted the $|\nabla\theta|^2$ term in their analytical investigation of a stationary flat interface. This term was added in Ref. [6], for practical reasons, in order to solve the model numerically. We shall see that this term makes no qualitative difference in the properties of static grain boundaries. However, as shown in Sec. V A, the mobility of a grain boundary vanishes as $h^{1/2}$ when in the $h\to 0$ limit. Thus the extra term introduced by KWC seems to be *required* for grain boundaries to move.

Assuming relaxational dynamics for a nonconserved set of order parameters, we find the gradient flow equations

$$Q(\eta,\nabla\theta)\tau_\eta\frac{\partial\eta}{\partial t}=-\epsilon\frac{\delta\mathcal{F}}{\delta\eta}=\alpha^2\nabla^2\eta-f_\eta-g_\eta s|\nabla\theta|$$
$$-h_\eta\frac{\epsilon^2}{2}|\nabla\theta|^2, \quad (2a)$$

$$P(\eta,\nabla\theta)\tau_\theta\eta^2\frac{\partial\theta}{\partial t}=-\epsilon\frac{\delta\mathcal{F}}{\delta\theta}=\nabla\cdot\left[h\epsilon^2\nabla\theta+gs\frac{\nabla\theta}{|\nabla\theta|}\right], \quad (2b)$$

where we use the subscripts to denote differentiation except for the time constants τ_η and τ_θ. The mobility functions P and Q must be positive definite, continuous at $\nabla\theta=\mathbf{0}$, but are otherwise unrestricted. System (2) must be supplemented by initial and boundary conditions, and a rule that specifies the handling of the indeterminacy of the term $\nabla\theta/|\nabla\theta|$. This particular type of the singularity is generally handled in a theory of extended gradients. Reference [16] proves that there is indeed a unique way to prescribe the value of the right hand side of Eq. (2b) when $\nabla\theta=0$. While we do not wish to attempt to explain all of the details of Ref. [16], it is useful to summarize the ultimate conclusion of the mathematical analysis.

Thus let us define a collection $\{G_i\}$ of distinct connected regions where $\nabla\theta=0$. We shall refer to G_i as the interior of grain i. The essence of the method of dealing with the singularity is that the orientation θ must remain uniform in space in each G_i. Therefore, the right hand side of Eq. (2b) is chosen in to be uniform in G_i. This condition, along with the requirement that η, θ, and $\nabla\theta$ be continuous at the boundaries of G_i, uniquely determines the rotation rate of each grain (i.e., $\partial\theta/\partial t$ in each G_i) and the motion of its boundaries.

The above decomposition of the system into grains and grain boundaries immediately allows us to consider the rotation of these grains and the dynamics of their boundaries. This decomposition is nontrivial, and is a direct consequence of the structure of the solution and our interpretation of grain boundaries as the regions where $\nabla\theta$ is nonzero. Even though, kinematicly, grain rotation and grain boundary migration can be distinguished, both are manifestations of the evolution equations (2), and both are driven from the regions of nonzero gradient in the lattice orientation.

Reference [22] verifies numerically that typical solutions of the gradient flow system [Eq. (2)] indeed consist of a collection of connected regions G_i in which $\nabla\theta=0$ and $\eta\approx 1$ (grain interiors) separated by narrow regions (grain boundaries) in which the orientation θ changes smoothly between the neighboring grains. Thus, the grains rotate (θ changes in time uniformly in each grain), and grain boundaries migrate (see Fig. 1, adopted from Ref. [22]).

III. FORMAL ASYMPTOTICS

Having elucidated the general properties of the model, we now examine the sharp-interface limit, in order to extract the physical quantities from our phase field model. As discussed earlier, solutions to the extended gradient flow system [Eqs. (2)] consist of grains in which $\nabla\theta=0$ separated by a network grain boundaries in which $\nabla\theta\neq 0$. Although no rigor-

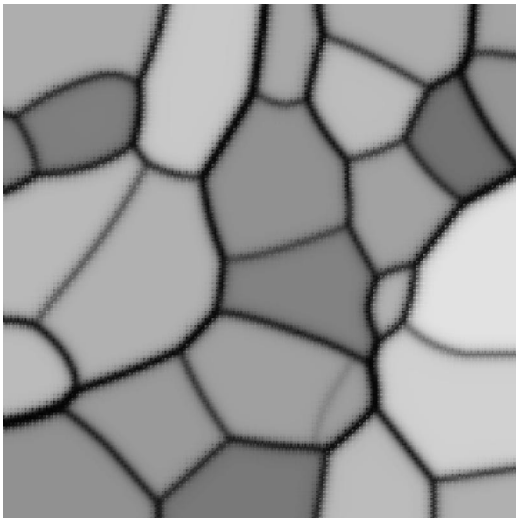

FIG. 1. Two-dimensional simulation of Eqs. (2) with simple choices for the couplings. The orientation θ is constant in the shaded grain regions. The shades of gray are used to represent the value of θ.

ous proof of the inevitability of this solution structure exists, there are two plausibility arguments. First, once this structure develops, one can show that it will persist [16]. And second, such a solution can be explicitly found for a flat stationary interface between two grains shown schematically in Fig. 2. This case corresponds to the zeroth order of the formal asymptotic expansion, as we show in what follows.

Figure 2 is highly suggestive. We have a bicyrstalline system with a localized region where properties change (i.e., the grain boundary). Let us therefore consider the $\epsilon \to 0$ limit of the gradient flow system (2). We expect the width of the grain boundary region to shrink to zero. In order that we obtain a more intuitive feel for precisely how the boundary region shrinks to zero width, it is useful to perform a heuristic analysis of the free energy. According to the arguments of Ref. [23], the width of the region of significant change in η is set by the competition of the first and second terms in the free energy [Eq. (1)]. Specifically, this width scales as $\alpha/\sqrt{f_{\eta\eta}}$. The width of the region, defined by $\nabla\theta \neq 0$, is set by the competition of the third and fourth terms in the free energy. In this case the width scales like $\epsilon^2 \Delta\theta/s$, where $\Delta\theta$ is the jump in θ across the interface (see Fig. 2). As discussed below, the scaling of α and s are chosen to ensure that both of these widths scale like $O(\epsilon)$ in the $\epsilon \to 0$ limit.

We employ the standard method of matched asymptotics [20], which uses the small ratio of the interface width to its radius of curvature as an expansion parameter. In this limit,

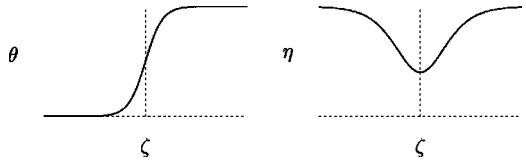

FIG. 2. A schematic representation of the solution for a flat static interface between two grains. ζ is the coordinate normal to the interface.

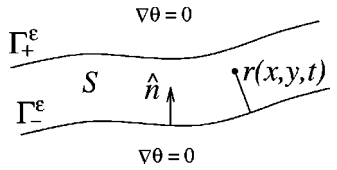

FIG. 3. The region S between the curves Γ_-^ϵ and Γ_+^ϵ in which $\nabla\theta \neq 0$.

all functions and their derivatives vary slowly along the interface compared to their variation across the interface. The analysis can therefore be advanced by defining a coordinate normal to the interface, and scaling it by ϵ. The order parameters as functions of this new coordinate are termed the inner solution. They are expanded into a power series in ϵ, and the resulting hierarchy of equations is solved order by order, subject to a matching condition with the outer solution. This outer solution, obtained by setting ϵ to zero, is valid far away from the interface.

The mathematics of the sharp interface limit of our model is atypical because the fields η and θ obey two different sets of equations [16]. Equations (2) hold in the grain boundary region which is defined as a strip S between two smooth nonintersecting curves $\Gamma_+^\epsilon(t)$ and $\Gamma_-^\epsilon(t)$ (see Fig. 3). Outside this strip, $\nabla\theta = 0$ and

$$Q\tau_n \frac{\partial \eta}{\partial t} = \alpha^2 \nabla^2 \eta - f_\eta. \tag{3}$$

Following Ref. [24], let us adopt curvilinear orthogonal coordinate system $\{r(x,y,t), \sigma(x,y,t)\}$. Let $r(x,y,t)$ be the distance of the point (x,y) in S from Γ_-^ϵ. On Γ_-^ϵ, coordinate σ is the arc length. We introduce a scaled variable $\zeta = r/\epsilon$, and expand η and θ in a formal power series in ϵ:

$$\eta(\zeta,\sigma,t) = \eta_0(\zeta,\sigma,t) + \epsilon\eta_1(\zeta,\sigma,t) + \cdots, \tag{4a}$$

$$\theta(\zeta,\sigma,t) = \theta_0(\zeta,\sigma,t) + \epsilon\theta_1(\zeta,\sigma,t) + \cdots. \tag{4b}$$

This expansion is valid in S and its immediate neighborhood. Also [20],

$$\nabla = \hat{n}\frac{1}{\epsilon}\frac{\partial}{\partial\zeta} + \hat{t}\frac{\partial}{\partial\sigma}, \tag{5a}$$

$$\nabla^2 = \frac{1}{\epsilon^2}\frac{\partial^2}{\partial\zeta^2} + \frac{\kappa}{\epsilon}\frac{\partial}{\partial\zeta} + O(1), \tag{5b}$$

$$\frac{\partial}{\partial t} = -\frac{v}{\epsilon}\frac{\partial}{\partial\zeta} + O(1), \tag{5c}$$

where $\hat{n}$ is the unit vector normal to Γ_-^ϵ pointing toward S (ζ increases in the direction of $\hat{n}$), and $\hat{t} \perp \hat{n}$ is the unit vector along the lines of constant r. The curvature $\kappa = \nabla^2 r$ is positive when $\hat{n}$ points away from the center of curvature of Γ_-^ϵ. The normal velocity $v = -\partial r/\partial t$ is positive when the interface moves in the direction of $\hat{n}$. This configuration is shown in Fig. 3.

In order to proceed, we must fix the scaling of α, s, τ_η, and τ_θ in the sharp interface limit. We select the scaling for which (1) a flat interface does not move, and (2) all terms in the free energy [Eq. (1)] scale with the same power of ϵ. We also assume that the mobility functions P and Q are independent of ϵ in the sharp interface limit (P need only be independent of ϵ in the grain boundary). These conditions fix

$$\alpha=\epsilon\tilde{\alpha},\quad s=\epsilon\tilde{s},\quad \tau_\eta=\epsilon^2\tilde{\tau}_\eta,\quad \tau_\theta=\epsilon^2\tilde{\tau}_\theta. \tag{6}$$

The final ingredient of the formal asymptotic analysis is the matching of the inner and outer solutions. The inner solution is found separately in the grain boundary $S(\nabla\theta\neq 0)$ and in its immediate neighborhood ($\nabla\theta=0$). The inner solution valid in S is denoted by $\eta(\zeta,\sigma,t)$ and $\theta(\zeta,\sigma,t)$ without superscripts. The piece of the inner solution valid in the interior of a grain just outside of S is denoted by $\eta^{(i)}(\zeta,\sigma,t)$ and $\theta^{(i)}(\zeta,\sigma,t)$. It is matched with the outer solution $\eta=1$ and $\theta=$const for $\zeta\to\infty$. We must also match the two pieces of the inner solution and their derivatives at the boundaries $\Gamma^\epsilon_\pm$ of the strip S, which are at $\zeta=\zeta_\pm$.

IV. ZEROTH ORDER SOLUTIONS: INTERFACE WIDTH AND ENERGY

Now, having detailed the formal method of asymptotic expansion, we proceed to examine the results of this expansion term by term. We begin, naturally enough, with the zeroth order. The ultimate result of the zeroth order calculation with be a determination of (i) the interface width, (ii) the surface energy, and (iii) the value of the order parameter η in grain boundary.

Without loss of generality we can shift the origin of ζ so that it is in the middle of S, $\zeta_\pm=\pm(\zeta_0+\epsilon\zeta_1+\cdots)$. We first look at the grain interior region $\zeta>\zeta_+$. Substituting the scaling ansatz [Eq. (6)] and the ϵ expansion [Eq. (4)] into Eq. (2), and using Eq. (5), we obtain

$$0=\tilde{\alpha}^2(\eta_0^{(i)})''-f_\eta(\eta_0^{(i)}),\quad (\theta_0^{(i)})'=0. \tag{7}$$

These solutions must be matched with the outer solutions $\eta=1$ and $\theta=\theta_+$, as $\zeta\to+\infty$. Since the zeroth order functions η_0 and θ_0 are independent of σ, the coordinate along the interface, and time t, they describe a flat stationary interface. They should therefore be symmetric with respect to the center of the boundary $\zeta=0$. We can thus set $\theta_+=\Delta\theta/2$, half the total misorientation (which is in general a function of time). Using the fact that $f(1)=0$, we arrive at

$$(\eta_0^{(i)})'=\frac{\sqrt{2f(\eta_0^{(i)})}}{\tilde{\alpha}},\quad \theta_0^{(i)}=\frac{\Delta\theta}{2}. \tag{8}$$

After similar manipulations we obtain the equations valid in S for $\zeta\in[-\zeta_+,\zeta_+]$:

$$0=\tilde{\alpha}^2\eta_0''-f_\eta(\eta_0)-\tfrac{1}{2}h_\eta(\eta_0)(\theta_0')^2-\tilde{s}g_\eta(\eta_0)\theta_0', \tag{9a}$$

$$0=[h(\eta_0)\theta_0'+\tilde{s}g(\eta_0)]'. \tag{9b}$$

Note that we assumed that $\theta'>0$ in S. This assumption proves to be unrestrictive, since all measurable quantities depend on the square of this derivative.

To obtain the boundary conditions for η_0 and θ_0, we employ two ideas. First, due to the aforementioned symmetry, η_0 is even and θ_0 is odd in ζ. Second, the requirement that η, θ, and their derivatives be continuous at $\zeta=\zeta_+$ can be shown to lead to the continuity of all terms in the ϵ expansion [Eq. (4)] at $\zeta=\zeta_0$. We thus obtain

$$\eta_0'(0)=0,\quad \eta_0'(\zeta_0)=\frac{\sqrt{2f(\eta_{\max})}}{\tilde{\alpha}}, \tag{10}$$

$$\theta_0(0)=0,\quad \theta_0(\zeta_0)=\frac{\Delta\theta}{2},\quad \theta_0'(\zeta_0)=0, \tag{11}$$

where $\eta_{\max}\equiv\eta_0(\zeta_0)$. Let us also introduce $\eta_{\min}\equiv\eta_0(0)$. This designation reflects our assumption that $\eta_0'>0$ in $\zeta\in[0,\zeta_0]$ so that $\eta_{\min}\leqslant\eta\leqslant\eta_{\max}$. We can prove that, in particular cases, this assumption is indeed justified.

Using the last boundary condition, we integrate Eq. (9b) to obtain

$$\theta_0'=\tilde{s}\frac{g(\eta_{\max})-g(\eta_0)}{h(\eta_0)}. \tag{12}$$

Upon substitution of this expression into Eq. (9a), we discover that η_0' is an integrating factor. Using the second condition in Eq. (10) we obtain

$$\eta_0'=\frac{1}{\tilde{\alpha}}\left[2f-\tilde{s}^2\frac{[g(\eta_{\max})-g]^2}{h}\right]^{1/2}. \tag{13}$$

The first condition in Eq. (10) furnishes the relation between $\eta_{\min}$ and $\eta_{\max}$:

$$g(\eta_{\max})=g(\eta_{\min})+\frac{\sqrt{2f(\eta_{\min})h(\eta_{\min})}}{\tilde{s}}. \tag{14}$$

Armed with this condition, we can obtain an equation for $\eta_{\min}$ via

$$\frac{\Delta\theta}{2}=\int_0^{\zeta_0}d\zeta\,\theta_0'=\tilde{\alpha}\tilde{s}\int_{\eta_{\min}}^{\eta_{\max}}d\eta\,\frac{g(\eta_{\max})-g}{h\sqrt{2f-\tilde{s}^2[g(\eta_{\max})-g]^2/h}}, \tag{15}$$

where we took advantage of the monotonicity of η_0. Once $\eta_{\min}$ is found, we can calculate the width of the boundary,

$$\zeta_0=\tilde{\alpha}\int_{\eta_{\min}}^{\eta_{\max}}\frac{d\eta}{\sqrt{2f-\tilde{s}^2[g(\eta_{\max})-g]^2/h}}, \tag{16}$$

and the interfacial energy

$$\gamma=\tilde{s}\Delta\theta g(\eta_{\max})+2\tilde{\alpha}\int_{\eta_{\max}}^{1}d\eta\sqrt{2f}$$

$$+2\tilde{\alpha}\int_{\eta_{\min}}^{\eta_{\max}}d\eta\sqrt{2f-\tilde{s}^2[g(\eta_{\max})-g]^2/h}. \quad (17)$$

These formulas reduce the flat boundary problem to quadratures. We are able to compute $\eta_{\min}$ and $\eta_{\max}$ from Eqs. (14) and (15), the interface width from Eq. (16), and the surface energy from Eq. (17).

As useful as these expressions are, insight can be better obtained from analytical expressions, since the above four equations must typically be solved numerically. Thus let us examine the behavior of the zeroth order solution in certain limits in which an approximate solution can be found. The integral on the right hand side of Eq. (15) can be calculated approximately when it is small. We identify two such situations.

A. Small h approximation to the zeroth order solution

To make contact with Ref. [5], in which the $|\nabla\theta|^2$ term in the free energy is set to zero, we consider a limit in which its coefficient vanishes $h\to 0$. Expanding Eq. (14) in powers of h we obtain, to lowest order,

$$\eta_{\max}-\eta_{\min}\approx\frac{\sqrt{2f^{\min}h^{\min}}}{\tilde{s}g_{\eta}^{\min}}\equiv G\ll 1, \quad (18)$$

where $f^{\min}\equiv f(\eta_{\min})$, etc. Thus, as $h\to 0$, the difference between $\eta_{\min}$ and $\eta_{\max}$ vanishes, while they remain well separated from 1. Therefore, f, g, and h and their derivatives are regular at the undistinguished point $\eta_{\min}<1$.

Let us define an auxiliary parameter y via $\eta=\eta_{\min}+Gy$, and expand Eq. (15) in powers of G. We obtain

$$\frac{\Delta\theta}{2}\approx\frac{\tilde{\alpha}}{s}\frac{\sqrt{2f^{\min}}}{g_{\eta}^{\min}}\int_0^1 dy\frac{1-y}{\sqrt{y(2-y)}}=\frac{\tilde{\alpha}}{\tilde{s}}\frac{\sqrt{2f^{\min}}}{g_{\eta}^{\min}}. \quad (19)$$

One could in principle now invert Eq. (19) to solve for $\eta_{\min}$. The width of the boundary ζ_0 can be then found with the same accuracy:

$$\zeta_0\approx\frac{\pi}{2}\frac{\tilde{\alpha}}{\tilde{s}}\frac{\sqrt{h^{\min}}}{g_{\eta}^{\min}}\to 0. \quad (20)$$

The interfacial energy is, in this same approximation,

$$\gamma\approx\tilde{s}g^{\min}\Delta\theta+2\tilde{\alpha}\int_{\eta_{\max}}^{1}d\eta\sqrt{2f}. \quad (21)$$

For a special case examined in Ref. [5], $f=\frac{1}{2}(1-\eta)^2$, $g=\eta^2$, and $h=0$, and Eq. (19) is easily invertible. Indeed, the expressions for $\eta_{\min}$ and γ coincide with those of Ref. [5].

We finally remark that within this approximation, the behavior of γ and ζ_0 in the limit of small misorientation $\Delta\theta$ depends on the properties of g and h near $\eta=1$. To see why this is true, let us look at Eq. (19) in the limit of small $\Delta\theta$. Unless g_{η} is singular at some value of η other than 1 (unphysical), small $\Delta\theta$ implies small $1-\eta_{\min}$ since $f(1)=0$. We shall see in Sec. IV B that it is true in general. This fact is not surprising, since small angle boundaries can be thought of as arrays of distant dislocations.

B. Small $\Delta\theta$ approximation to the zeroth order solution

All parameters being fixed, the right hand side of Eq. (15) can be small if and only if

$$\rho\equiv\eta_{\max}-\eta_{\min}\ll 1. \quad (22)$$

Since $f(1)=0$, it is clear from Eq. (14) that

$$\lambda\equiv 1-\eta_{\min}\ll 1. \quad (23)$$

Also, since we chose $f(1)=0$, we can approximate it by a parabola $f(\eta)\approx\frac{1}{2}f_{\eta\eta}(1)(1-\eta)^2$ near $\eta=1$. Then

$$\rho g_{\eta}^{\min}\approx\lambda\frac{\sqrt{f_{\eta\eta}(1)h^{\min}}}{\tilde{s}}. \quad (24)$$

If the behavior of g and h near $\eta=1$ is known, we can obtain a complete solution to the zeroth order problem in this limit. Instead, let us focus on the scaling of the interface width ζ_0 and the interfacial energy γ in the $\Delta\theta\to 0$ limit. This scaling can be deduced without a complete solution of the zeroth order problem.

Suppose that, near $\eta=1$ $(0<\lambda\ll 1)$,

$$g_{\eta}^{\min}\sim\lambda^{\beta},\quad h^{\min}\sim\lambda^{2\omega}. \quad (25)$$

Then, from Eq. (24), we obtain

$$\rho\sim\lambda^{1+\omega-\beta}. \quad (26)$$

Note that, since $\rho<\lambda$ by definition, the scaling exponent in Eq. (26) must be greater than or equal to 1. This means that, in this limit, the zeroth order solution exists only when $\omega\geqslant\beta$.

To determine the scaling of the right hand side of Eq. (15), we define a finite integration variable $y\in[0,1]$ via $\eta-\eta_{\min}=\rho y$. Then

$$d\eta\sim\rho\sim\lambda^{1+\omega-\beta}, \quad (27a)$$

$$\frac{g(\eta_{\max})-g}{h}\sim\rho\frac{g_{\eta}^{\min}}{h^{\min}}\sim\lambda^{1-\omega}, \quad (27b)$$

$$2f-\tilde{s}^2\frac{[g(\eta_{\max})-g]^2}{h}$$

$$=\frac{1}{h}[(2fh-2f^{\min}h^{\min})+2\tilde{s}(g-g^{\min})$$

$$\times\sqrt{2f^{\min}h^{\min}}-\tilde{s}^2(g-g^{\min})^2]\sim\lambda^{2+\beta-\omega}. \quad (27c)$$

We used the fact that $\omega\geqslant\beta$ to establish that the second term in the square brackets of Eq. (27c) dominates (when $\omega=\beta$

all three terms in these square brackets are equally important). Substituting scaling relations (27) into Eq. (15), we obtain

$$\Delta\theta \sim \lambda^{1+[(\omega-\beta)/2]}. \tag{28}$$

We are now ready to calculate the behavior of ζ_0 and γ in the $\Delta\theta \to 0$ limit. Substituting the scaling relations (27) into Eq. (16), we obtain

$$\zeta_0 \sim \lambda^{3/2(\omega-\beta)} \sim (\Delta\theta)^{[3(\omega-\beta)]/(2+\omega-\beta)}. \tag{29}$$

The interfacial energy consists of three pieces $\gamma = \gamma_1 + \gamma_2 + \gamma_3$, which scale differently with $\Delta\theta$. We list them separately:

$$\gamma_1 = 2\tilde{\alpha}\int_{\eta_{\min}}^{\eta_{\max}} d\eta \sqrt{2f - \tilde{s}^2[g(\eta_{\max}) - g]^2/h} \sim \lambda^{2+(3/2)(\omega-\beta)}, \tag{30a}$$

$$\gamma_2 = 2\tilde{\alpha}\int_{\eta_{\max}}^{1} d\eta \sqrt{2f} \sim \lambda^2 \sim (\Delta\theta)^{4/(2+\omega-\beta)}, \tag{30b}$$

$$\gamma_3 = \tilde{s}\Delta\theta g(\eta_{\max}) \sim g^{\min}\Delta\theta. \tag{30c}$$

We can make several observations. First, since $\omega \geqslant \beta, \gamma_2$ always dominates γ_1 in the $\Delta\theta \to 0$ limit. Second, when $\beta < -1$ we can integrate Eq. (25) to obtain $g^{\min} \sim \lambda^{1+\beta}$. When $\beta = -1$, in a similar fashion we obtain $g^{\min} \sim \ln\lambda$. For $\beta > -1$ the behavior of g near $\eta = 1$ is arbitrary. Thus the scaling of the interfacial energy (whether it is dominated by γ_2 or γ_3) in the limit of the small misorientation can be freely controlled by adjusting the behavior of g and h near $\eta = 1$.

V. FIRST ORDER SOLUTIONS: INTERFACE MOBILITY

Having completed our analysis of the zeroth order in the asymptotic expansion, we now continue on to first order. This order in the expansion will yield the velocity of the interface as a function of geometry, mobilities P and Q, and surface energy. From classical as well as order parameter models, we expect this motion to be by curvature [25], and, as we show below, this is indeed the case.

To begin, in order for us to establish the matching conditions between the two pieces of the first order solution, let us look at the equation for $\eta_1^{(i)}$ valid in $\zeta > \zeta_+$:

$$-[v\tilde{\tau}_\eta Q + \tilde{\alpha}^2\kappa](\eta_0^{(i)})' = \tilde{\alpha}^2(\eta_1^{(i)})'' - \eta_1^{(i)} f_{\eta\eta}(\eta_0^{(i)}). \tag{31}$$

Progress can be made by noting that $\eta_1^{(i)} = (\eta_0^{(i)})'$ is a solution of Eq. (31), with the left hand side set to 0. We can take advantage of this fact by multiplying Eq. (31) by $(\eta_0^{(i)})'$, and integrating over the grain interior. Using the matching condition with the outer solution, which states that all derivatives vanish as $\zeta \to \infty$, we obtain

$$\tilde{\alpha}^2[(\eta_1^{(i)})'(\eta_0^{(i)})' - \eta_1^{(i)}(\eta_0^{(i)})'']_{\zeta=\zeta_+} = \int_{\zeta_+}^{\infty} d\zeta [v\tilde{\tau}_\eta Q + \tilde{\alpha}^2\kappa][(\eta_0^{(i)})']^2. \tag{32}$$

As we mentioned above, all orders of the ϵ expansion and their derivatives must be continuous at ζ_+ or, equivalently, at ζ_0. Consequently, we may drop the (i) superscript from the expression on the left hand side of Eq. (32). This condition will suffice to set η_1 at $\zeta = \zeta_0$. We will not need the boundary condition for θ_1 at $\zeta = \zeta_0$.

Turning our attention to the boundary region $\zeta \in [0, \zeta_0]$, we write down the first order equations

$$-v\tilde{\tau}_\eta Q\eta_0' = \tilde{\alpha}^2(\eta_1'' + \kappa\eta_0') - f_{\eta\eta}\eta_1 - \frac{h_{\eta\eta}}{2}\eta_1(\theta_0')^2 - h_\eta\theta_0'\theta_1' - \tilde{s}g_{\eta\eta}\eta_1\theta_0' - \tilde{s}g_\eta\theta_1', \tag{33a}$$

$$-v\tilde{\tau}_\theta\eta_0^2 P\theta_0' = \tilde{s}\kappa g + \kappa h\theta_0' + [h\theta_1' + h_\eta\eta_1\theta_0' + \tilde{s}g_\eta\eta_1]', \tag{33b}$$

where we used the fact that $\nabla\cdot[\nabla\theta/|\nabla\theta|] = \kappa$. The couplings f, g, and h, and their derivatives, and Q and P in Eqs. (33) are evaluated at the zeroth order solution.

We can fix the boundary conditions at $\zeta = 0$ for the first order functions by noting that η_1 is odd while θ_1 is even in ζ. Therefore,

$$\eta_1(0) = 0, \quad \theta_1'(0) = 0. \tag{34}$$

Using the second condition we integrate Eq. (33b) to obtain

$$h(\eta_0)\theta_1' = -[h_\eta(\eta_0)\theta_0 + \tilde{s}g_\eta(\eta_0)]\eta_1 - \int_0^\zeta d\zeta' [v\tilde{\tau}_\theta P(\eta_0, \hat{n}\theta_0')\eta_0^2\theta_0' - \tilde{s}\kappa g(\eta_0) - \kappa h(\eta_0)\theta_0']. \tag{35}$$

Upon substitution of this expression into Eq. (33a), we obtain an equation for η_1 of the form

$$\mathcal{L}[\eta_1] \equiv \tilde{\alpha}^2\eta_1'' + C(\eta_0, \theta_0)\eta_1 = D(\eta_0, \theta_0), \tag{36}$$

where

$$D(\eta_0, \theta_0) = -\eta_0'(v\tilde{\tau}_\eta Q + \kappa) - \frac{h_\eta\theta_0' + \tilde{s}g_\eta}{h} \times \int_0^\zeta d\zeta' [v\tilde{\tau}_\theta P\eta_0^2\theta_0' + \kappa(h\theta_0' + \tilde{s}g)]. \tag{37}$$

The exact form of C is unimportant, since we can show by direct substitution that (as in a conventional asymptotic expansion problem) $\mathcal{L}[\eta_0'] = 0$. This fact can be utilized to obtain a solvability condition which determines the velocity of the interface v. Multiplying Eq. (36) by η_0', and integrating over $[0, \zeta_0]$, we obtain

$$\tilde{\alpha}^2[\eta_0'\eta_1' - \eta_0''\eta_1]_0^{\zeta_0}$$

$$= \tilde{\alpha}^2[(\eta_1^{(i)})'(\eta_0^{(i)})' - \eta_1^{(i)}(\eta_0^{(i)})'']_{\zeta=\zeta_0}$$

$$= \int_{\zeta_0}^{\infty} d\zeta [v\tilde{\tau}_\eta Q + \tilde{\alpha}^2\kappa][(\eta_0^{(i)})']^2$$

$$= -\int_0^{\zeta_0} d\zeta [v\tilde{\tau}_\eta Q + \tilde{\alpha}^2\kappa](\eta_0')^2$$

$$-\int_0^{\zeta_0} d\zeta\, \theta_0'[v\tilde{\tau}_\theta P \eta_0^2\theta_0' + \kappa(h\theta_0' + \tilde{s}g)]. \tag{38}$$

Solving for the interface velocity v, and using Eqs. (12), (13), and (17), yields

$$v = -\kappa\gamma\mathcal{M}. \tag{39}$$

As expected, v is proportional to both the curvature and the energy of the interface. The mobility is given by

$$\frac{1}{\mathcal{M}} = \tilde{\tau}_\eta \int_0^{\infty} d\zeta\, Q(\eta_0, \hat{n}\theta_0')(\eta_0')^2$$

$$+ \tilde{\tau}_\theta \int_0^{\infty} d\zeta\, P(\eta_0, \hat{n}\theta_0')\eta_0^2(\theta_0')^2. \tag{40}$$

We dropped the superscript (i), since it is clear that solutions which are valid in the grain interior should be used in Eq. (40) for $\zeta > \zeta_0$.

Just as in a conventional formal asymptotic analysis, we obtained the normal velocity of the interface without having to solve the first order equations. This is a general feature of analyses of this kind, and allows one to express the mobility of the interface in terms of the properties of a stationary interface. To better understand the behavior of the interface mobility $\mathcal{M}$, let us apply the approximations of Secs. IV A and IV B to Eq. (40).

A. Mobility in the small *h* limit

To illustrate the importance of the $|\nabla\theta|^2$ term in the free energy for the motion of boundaries, let us again consider the limit in which its coefficient h vanishes. The second term in Eq. (40) dominates in this limit. Assuming for the sake of the argument that P does not depend on $\nabla\theta$, we obtain

$$\frac{1}{\mathcal{M}} \approx \frac{\pi\tilde{\tau}_\theta\tilde{\alpha}}{2\tilde{s}} \frac{P^{\min}\eta_{\min}^2 f^{\min}}{g_\eta^{\min}\sqrt{h^{\min}}} \to \infty. \tag{41}$$

The mobility of the grain boundary therefore vanishes as $h^{1/2}$ in this limit, in support of our claim that the $|\nabla\theta|^2$ term is required for migration of boundaries.

B. Mobility in the small $\Delta\theta$ limit

It is instructive to trace the behavior of the interface mobility in the limit of vanishing misorientation. For simplicity, we assume here that the mobility functions P and Q are regular, and assume a nonzero value at $\eta=1$ and $\nabla\theta=0$. Using Eq. (27), we obtain the scaling of the three pieces which make up the right hand side of Eq. (40):

$$\int_0^{\zeta_0} d\zeta\, Q(\eta_0')^2 \sim \lambda^{2+\omega-\beta}, \tag{42a}$$

$$\int_{\zeta_0}^{\infty} d\zeta\, Q(\eta_0')^2 \sim \lambda^{2+[(\beta-\omega)/2]}, \tag{42b}$$

$$\int_0^{\zeta_0} d\zeta\, P\eta_0^2(\theta_0')^2 \sim \lambda^{2-[(\omega+3\beta)/2]}. \tag{42c}$$

Equation (28) can now be used to determine the behavior of $\mathcal{M}$ in the $\Delta\theta\to 0$ limit. We obtain

$$\frac{1}{\mathcal{M}} \sim \begin{cases} (\Delta\theta)^{(4-\omega-3\beta)/(2+\omega-\beta)}, & \beta > 0 \\ (\Delta\theta)^{(4-\omega+\beta)/(2+\omega-\beta)}, & \beta \leqslant 0. \end{cases} \tag{43}$$

To illustrate, if g and h are regular at $\eta=1$ so that $\omega=\beta=0$, our analysis yields $\gamma\sim\Delta\theta$, while $\mathcal{M}^{-1}\sim(\Delta\theta)^2$, so that the interface velocity diverges in the limit of vanishing misorientation $v\sim(\Delta\theta)^{-1}$.

VI. GRAIN ROTATION

As we discussed above, this model also allows for the grains to rotate. Let us consider a fully developed grain structure. In the sharp interface limit, the solution consists of a set of regions G_i of spatially uniform θ (grains) separated by narrow (or order ϵ) grain boundaries. To calculate the rotation rate Ω_i of grain i, we integrate Eq. (2b) over the grain interior G_i. We obtain

$$\Omega_i\tau_\theta \int_{G_i} dA\, \eta^2 P(\eta,0) = s \oint_{\partial G_i} d\sigma\, g(\eta)\hat{n}\cdot\left[\frac{\nabla\theta}{|\nabla\theta|}\right]$$

$$\approx s\sum_j \zeta_{ij} g(\eta_{\max}^{ij})\,\mathrm{sgn}(\Delta\theta_{ij}). \tag{44}$$

Here ζ_{ij} is the length of the common boundary between grains i and j. The summation is over the neighboring grains j of orientation θ_j. In integrating by parts, we used the continuity of $\mathbf{b}\equiv\nabla\theta/|\nabla\theta|$ at the edge of the grain [16]. In the grain boundary S, $\mathbf{b}$ is a unit vector in the direction of increasing θ. Thus, away from a triple junction, $\mathbf{b}=\hat{n}_{ij}\,\mathrm{sgn}(\Delta\theta_{ij})$ on both edges $\Gamma_\pm^\epsilon$ of the boundary between grains i and j. The unit normal $\hat{n}_{ij}$ points from grain i to grain j. The periodicity of θ must be taken into account to calculate $\mathrm{sgn}(\Delta\theta_{ij})$.

Let us examine the scaling of the rotation rate Ω_i in the sharp interface limit. The right hand side of Eq. (44) scales as ϵ. For Ω_i to be finite and nonzero in the sharp interface limit, the left hand side

$$\tau_\theta \int_{G_i} dA\, \eta^2 P(\eta,0), \tag{45}$$

must also scale like ϵ. Recall that η is exponentially close to 1 in all of G_i except a narrow (of order ϵ) strip near the

boundary. Therefore, if P is independent of ϵ and has neither a zero nor a singularity at $\eta=1$, then Eq. (45) is approximately equal to $A_i P(1,0)$, where A_i is the area of the ith grain. Therefore, in the sharp interface limit, $\Omega_i \sim s/\tau_\theta \sim 1/\epsilon$. We therefore reach a conclusion that when P is regular at $\eta=1$, grain rotation dominates grain boundary migration in the sharp interface limit. The reason for this result is that $\partial\theta/\partial t$ is continuous across the edge of the grain boundary. Inside the grain boundary, this time derivative must scale with the inverse of the grain boundary width $1/\epsilon$. The time rate of change of the orientation θ in the grain interior must therefore have the same scaling.

Another way of interpreting the divergence of the rotation rate in the sharp interface limit is to consider what happens in the interior of the grain. Since the orientation order parameter is constrained to remain uniform in space, it may be thought of as obeying a diffusion equation with infinite diffusivity. It is therefore not surprising that for a generic choice of the mobility function P, the rotation rate is of the same order as the rate of change of θ in the grain boundaries (fast).

However, there exist special choices for P which ensure that the rotation rate does not diverge in the sharp interface limit. This can be accomplished by letting the P diverge like $1/\epsilon$ in the grain interior. (Relaxing the constraint that P be independent of ϵ in the grain interior does not alter the results of the asymptotic expansion, since the dynamics of θ in the interior of the grain is slaved to its behavior in the grain boundary.)

For example, by choosing

$$P(\eta,\nabla\theta)=\begin{cases} 1, & \nabla\theta\neq 0 \\ \epsilon^{\mu-1}[\ln(1-\eta)]^{\mu}, & \nabla\theta=0, \end{cases} \tag{46}$$

where $\mu\neq -1$, we ensure that $P\sim 1/\epsilon$, as we show by calculating $\eta_0^{(i)}$ below. This choice of P is plausible. When material is nearly a perfect crystal (η close to 1), i.e., there are few defects, one should expect the rate at which the order parameters change to vanish.

Integral (45) may be now calculated approximately in the sharp interface limit. We first calculate $\eta_0^{(i)}$ far away from the boundary, where it is close to 1. Using the approximation for $f\approx \frac{1}{2} f_{\eta\eta}(1)(1-\eta)^2$, we obtain

$$1-\eta_0^{(i)} \sim \exp\left(-\frac{\sqrt{f_{\eta\eta}(1)}}{\tilde{\alpha}}\zeta\right). \tag{47}$$

Focusing on the ϵ scaling in the sharp interface limit, we deduce that integral (45) scales as

$$\tau_\theta \epsilon^{\mu-1}\int_{G_i} dA\ \eta^2[\ln(1-\eta)]^{\mu} \sim L\epsilon^{2+\mu}\int^{L/\epsilon}\zeta^{\mu}d\zeta \sim L^{2+\mu}\epsilon, \tag{48}$$

which, as we desired, is proportional to ϵ. The rotation rate Ω_i is thus finite in the sharp interface limit.

Another important consequence of this argument is that since the perimeter of a grain is proportional to L, the right hand side of Eq. (44) scales as L, and we can determine the dependence of the rotation rate of a grain on its perimeter:

$$\Omega \sim \frac{1}{L^{1+\mu}}. \tag{49}$$

This prediction is independent of the choice of other the model functions. With an appropriate choice of μ, it can be consistent with the heuristic derivations [15,26] of the rotation rate due to the diffusion of atoms along the grain boundary. These studies obtain a $1/L^3$ or $1/L^4$ scaling of Ω depending on the mechanism. In a separate study, Martin [12] assumed that rotation is caused by viscous motion of dislocations, and obtained a rotation rate which was independent of L.

VII. APPROXIMATE MODEL OF A SINGLE CIRCULAR GRAIN

To illustrate the predictions of the sharp interface limit calculation of the preceding sections, we consider a circular grain of radius R and orientation θ embedded in an immovable matrix of orientation 0. To make analytical progress, we choose $Q=1$, $P=-\ln(1-\eta)$, $f=\frac{1}{2}(1-\eta)^2$, $g=-2\eta-2\ln(1-\eta)$, and $h=1$, to ensure a finite rotation rate in the sharp interface limit and Read-Shockley [27] behavior for low angle boundaries. We also restrict ourselves to the small θ approximation. In this limit we can carry out the expansion in detail, to obtain

$$\gamma \approx \tilde{s}\theta\left(1-\ln\frac{\tilde{s}\theta}{\tilde{\alpha}}\right), \quad \zeta_0 \approx \frac{\pi}{4}\left(\frac{\tilde{\alpha}\theta}{\tilde{s}}\right)^{1/2}, \quad \frac{1}{\mathcal{M}} \approx \frac{\tilde{\tau}_\eta \tilde{s}\theta}{2\tilde{\alpha}^2}. \tag{50}$$

Applying the motion by curvature result (39), we obtain

$$2R\dot{R} \approx a_1 \ln\theta, \tag{51}$$

where $a_1=4\tilde{\alpha}^2/\tilde{\tau}_\eta$. The expression for the rotation rate with the radius of the grain R and misorientation θ can be obtained via the arguments of Sec. VI. We obtain

$$\dot{\theta} \approx a_2 \frac{\ln\theta}{R^2}, \tag{52}$$

where $a_2=6\tilde{s}\tilde{\alpha}/\tilde{\tau}_\theta$. Solutions to these equations for $R(0)=1$ and $\theta(0)=0.1$ are given in Figs. 4 and 5. The ratio a_1/a_2 controls the behavior of the solution. When this ratio is small, rotation dominates the dynamics, so that the radius of the grain is not significantly reduced by the time the grain rotates into alignment with the matrix. On the other hand, when this ratio is large, the evolution of the radius squared of the grain is almost linear in time, as in the case of the motion by curvature.

Comparison with molecular a dynamics simulation of Upmanyu and Srolovitz reveals that our simple model is sufficiently accurate and flexible to predict the behavior of a circular grain whose misorientation is near a special value. Upmanyu and Srolovitz found that near a special misorientation, such that the number of coincident lattice sites is large

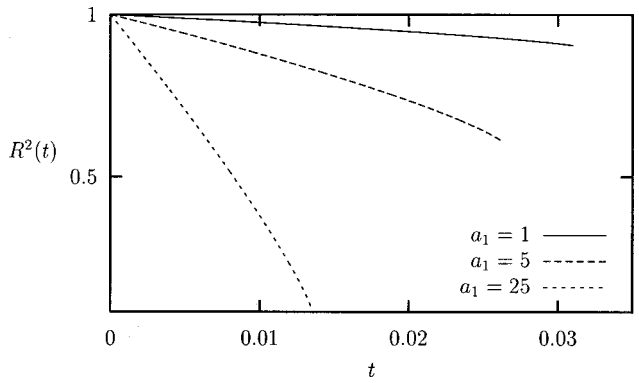

FIG. 4. Evolution of the squared radius $R^2(t)$ of the circular grain for $a_2=1$ and three values of a_1.

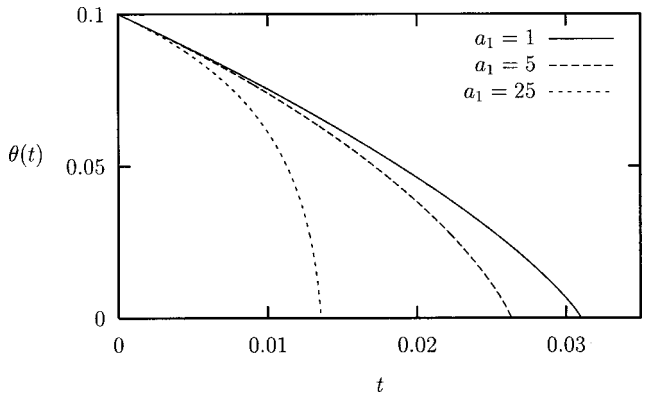

FIG. 5. Evolution of the orientation $\theta(t)$ of the circular grain for the same three values of a_1.

(e.g., $\Sigma 5$), the energy of the grain boundary as a function of the misorientation has a cusp, while its mobility has a sharp peak. Grains whose initial misorientation is close to a special value rotate toward that special misorientation.

VIII. DISCUSSION

In this paper we analyze a modified version of the phase field model of KWC [6]. This model is constructed to describe rotation of crystalline grains coupled to the motion of grain boundaries. The order parameter θ reflects the local crystal orientation, whereas η represents local crystalline order. The Ginzburg-Landau free energy depends only on $\nabla\theta$, and is therefore invariant under rotations. Inclusion of the nonanalytic $|\nabla\theta|$ term into the free energy results in singular gradient flow equations. However, this singularity can be dealt with in a systematic way.

Quite generally, solutions to the model represent a collection of regions of uniform θ—grains—connected by narrow (or order ϵ) internal layers—grain boundaries. We are able to calculate the velocity of the boundaries in the limit of vanishing interface thickness, and find that it is proportional to the product of surface energy, curvature of the interface, and a mobility which depends on model parameters. The behavior of the interfacial width, energy, and mobility in the limit of the small misorientation is controlled by the behavior of the model couplings near $\eta=1$.

We calculate the rate of grain rotation in the sharp interface limit, and find that the mobility function P must diverge as $1/\epsilon$ in the interior of the grain to ensure that the rotation rate is finite in this limit. We explain this mathematical requirement by noting that the singular term in the free energy results in infinitely fast diffusion in the interior of a grain. Therefore, the mobility function P must compensate for that fact. We suggest a choice P which results in a finite rotation rate.

For a plausible choice of model functions, motivated by the physics of low angle grain boundaries, we derive and solve equations describing a circular grain embedded in a matrix. We find that, as expected, when the scaled coefficient $\tilde{s}$ of the $|\nabla\theta|$ term in the free energy is large, rotation is fast, so that the radius of the grain does not change much by the time the grain rotates into coincidence with the matrix. When $\tilde{s}$ is small, rotation becomes important only when the radius is significantly reduced.

We conclude by remarking that the model may be readily generalized in a variety of ways. We may extend the model to three dimensions, by constructing an appropriate tensor order parameter which reflects the symmetries of the lattice. Anisotropy may be included by allowing the coefficient of the $|\nabla\eta|^2$ term to depend on $\nabla\theta$. Alternatively, the mobility functions may be made anisotropic to yield kinetics which depend on the orientation of the boundary region. Overall, this model will provide a foundation for a physical, yet still relatively mathematically simple, model of grain boundary evolution and grain rotation.

[1] B. Morin, K. R. Elder, M. Sutton, and M. Grant, Phys. Rev. Lett. **75**, 2156 (1995).
[2] M. T. Lusk, Proc. R. Soc. London, Ser. A **455**, 677 (1999).
[3] L. Q. Chen and W. Yang, Phys. Rev. B **50**, 15 752 (1994).
[4] V. Tikare, E. A. Holm, D. Fan, and L. Q. Chen, Acta Mater. **47**, 363 (1998).
[5] R. Kobayashi, J. A. Warren, and W. C. Carter, Physica D **140**, 141 (2000).
[6] R. Kobayashi, J. A. Warren, and W. C. Carter, Physica D **140**, 141 (2000).
[7] J. A. Warren, R. Kobayashi, and W. C. Carter, J. Cryst. Growth **211**, 18 (2000).
[8] J. B. Collins and H. Levine, Phys. Rev. B **31**, 6119 (1985).
[9] G. Caginalp, in *Applications of Field Theory to Statistical Mechanics*, edited by L. Garrido (Springer, Berlin, 1985), p. 216.
[10] J. S. Langer, in *Directions in Condensed Matter Physics*, edited by G. Grinstein and G. Mazenko (World Scientific, Philadelphia, 1986), p. 164.
[11] J. C. M. Li, J. Appl. Phys. **33**, 2958 (1961).
[12] G. Martin, Phys. Status Solidi B **172**, 121 (1992).
[13] J. W. Cahn, in *Sintering of Advanced Ceramics*, edited by C. A. Handwerker and J. E. Blendell (American Ceramics Society, Westerville, OH, 1990), pp. 185–194.

[14] K. E. Harris, V. V. Singh, and A. H. King, Acta Mater. **46**, 2623 (1998).
[15] S.-W. Chen and R. W. Balluffi, Acta Metall. **34**, 2191 (1986).
[16] R. Kobayashi and Y. Giga, J. Stat. Phys. **95**, 1187 (1999).
[17] J. E. Taylor, J. W. Cahn, and C. A. Handwerker, Acta Metall. Mater. **40**, 1443 (1992).
[18] G. Caginalp, Arch. Ration. Mech. Anal. **92**, 205 (1986).
[19] G. B. McFadden, A. A. Wheeler, R. J. Braun, S. R. Coriell, and R. F. Sekerka, Phys. Rev. E **48**, 2016 (1993).
[20] P. C. Fife, *Dynamics of Internal Layers and Diffusive Interfaces* (SIAM, Philadelphia, 1988), Chap. 1.
[21] U. Ebert and W. van Saarloos, Phys. Rep. **337(1–2)**, 139 (2000).
[22] R. Kobayashi and J. A. Warren (private communication).
[23] J. W. Cahn and J. E. Hilliard, J. Chem. Phys. **28**, 258 (1958).
[24] J. W. Cahn, C. M. Eliott, P. C. Fife, and O. Penrose (private communication).
[25] S. M. Allen and J. W. Cahn, Acta Metall. **27**, 1085 (1979).
[26] G. Gessinger, F. V. Lenel, and G. S. Ansell, Scr. Metall. **2**, 547 (1968).
[27] W. T. Read and W. Shockley, Phys. Rev. **78**, 275 (1950).